Design optimization of the parallel-feeding multi-effect evaporation system using multi-objective genetic algorithm

Cong Liu, Mingshu Bi*, Guangrui Cui

School of Chemical Machinery, Dalian University of Technology, 116023, China, emails: bimsh@dlut.edu.cn (M. Bi), costaliugame@main.dlut.edu.cn (C. Liu), cuiguangrui.xuexi@foxmail.com (G. Cui)

ABSTRACT

Multi-effect evaporation (MEE) system design is a complex task and affected by a series of variables. Design optimization of the parallel-feeding multi-effect evaporation system using a multi-objective genetic algorithm is studied in the paper. Gain output ratio (GOR) and simplified cost of water are considered as two objective functions and the number of the effect (n), the top brine temperature (T_b), the apparent temperature difference (Δt), and the recovery ratio of the first effect (RR_1) are defined as the input variables. It is found that for satisfying the objective function requirement the top brine temperature (T_b) and recovery ratio (RR_1) are always the upper limits of the simulation interval, which are 80°C and 4, respectively. Simultaneously, two design approaches DS and DTD and two evaluation criteria optimal yield and optimal economical are proposed to evaluate the various optimal solutions. Two case studies are presented to illustrate the optimization process and result selection in detail. The multi-objective genetic algorithm proposed in the paper not only can optimize the existing scheme but also can provide several scenarios with their advantages to decision-makers at the design process. The present study has demonstrated the successful application of a multi-objective genetic algorithm for the optimal design of parallel-feeding configuration.

Keywords: Parallel feed; Multi-effect evaporation; Design optimization; Multi-objective genetic algorithm

1. Introduction

Desalination is used to overcome freshwater scarcity in the countries and regions that lack freshwater [1]. In the desalination area, the predominant technologies are reverse osmosis (60%), multistage flash (MSF, 26%), and multi-effect evaporation (MEE, 8%) [2]. Although the market share of the multi-effect evaporation technology is not large, it is widely used in Gulf cooperation council countries due to its advantages of lower manufacturing requirements, simple pretreatment, lower startup time, and lower capital cost [3,4]. MEE process has different types and arrangements [5]. There are mainly three different types: forward, backward, and parallel feed [6]. Comparing the other two feeding configurations, parallel feed is considered the most reasonable configuration in industrial applications due to its high gain output ratios (GORs) and low fouling [6].

The parallel-feeding MEE (PF-MEE) is a complex system that consists of several evaporators, a series of feedwater preheaters, a train of flashing boxes, the last effect condenser, and a venting system [7]. The design of the PF-MEE needs to make each component a better match to achieve good performance. It involves input and debugging of a large number of variables to meet product requirements and a given set of design constraints.

The most famous literature about the design of the parallel-feed multi-effect evaporation system has been written by El-Dessouky et al. [8], and El-Dessouky and

* Corresponding author.

Ettouney [9]. Performance analysis for the parallel-feed MEE system was presented in the paper. They studied the effects of the heating steam temperature, intake seawater salinity, and the number of effects on the specific heat transfer area, the performance ratio, the specific flow rate of the cooling water, and the conversion ratio. Their research laid a good foundation, and other scholars improved in-depth based on their results. In Sharan and Bandyopadhyay's paper [5], a new methodology, based on the principle of process integration combined with mathematical optimization, is developed in this paper to determine the optimal feed flow rate for each effect. The results showed that the GOR for 12-effect MEE can be increased by 11% with an optimized feed flow rate. Darwish and Abdulrahim [10] studied a four-effect parallel-feed MEE system and presented the thermodynamic analysis. These analyses determine the temperature and salinity profiles of the system, the amount of vapor generated by boiling, and by flashing in each effect, the required heat transfer areas for the effects and feed heaters, the gain and recovery ratios, and cooling water to distillate ratio. With TVC technology development, a parallel-feed MEE system integrated with TVC is widely used. Much literature about the optimization design of MED-TVC has appeared. For reducing the power consumption and increasing GOR value, Kamali and Mohebinia [11] developed a general computer code for the MED-TVC. To validate program outputs, the results of this program were tested on an available MED system in Kish Island. It is concluded that this experience well proves program validity to the design and optimization of MED-TVC systems. Amer [12] developed a steady-state mathematic model of the MEE-TVC desalination system using Engineering Equations Solver (EES) to evaluate the model system performance. The model validity is examined against three commercial ME-TVC units, which showed good results. Onishi et al. [13,14] studied the process optimization for zero-liquid discharge desalination of shale gas flowback water under uncertainty. They introduced a new model for the synthesis of zero-liquid discharge desalination systems under different water flow rates and salinities. Jamil and Zubair [15] studied the effect of feed flow arrangement and the number of evaporators on the performance of multi-effect mechanical vapor compression desalination systems. Elsayed et al. [16,17] proposed an exergo-economic model to simulate the multi-effect with the thermal vapor compressor (MED-TVC) system. Al-Mutaz and Wazeer [6] proposed a mathematical model to study the effect of all the parameters on total capacity, gain output ratio, special heat transfer area, specific heat consumption, and the temperature difference between effects under different operating and design conditions. Zhou et al. [18] and Shen et al. [19] investigated the thermodynamic losses caused by the flow resistances and the boiling point elevation (BPE) in low-temperature multi-effect evaporation (LT-MEE) desalination plant. Some scholars used a particle swarm algorithm to optimize the multi-effect evaporation system with single-objective or multi-objective. Esfahani et al. [20] proposed a systematic approach of analysis and optimization of the multi-effect distillation-thermal vapor compression (MED-TVC) desalination system. The paper aiming the minimize TAC (total annual

cost) and maximize GOR and Q (freshwater flow), studied the effect of input variables, such as temperature difference, motive steam mass flow rate, and preheated feedwater temperature. Ameri and Jorjani [21] introduced an integrated organic Rankine cycle and a multi-effect desalination system. The fast and elitist non-dominated sorting genetic algorithm-II (NSGA-II) is applied to optimize the objective functions including distilled water production and the total cost rate (power generation price) simultaneously. Ben Ali and Kairouani [22] used genetic algorithms for optimization of operating parameters of recirculation multi-stage flash (MSF-BR) desalting plant, taking into consideration the change of brine heater fouling factor and seasonal variation of seawater temperature. Sayyaadi and Saffari [23] proposed an economical model that is applied to minimize the total revenue requirement using the single-objective genetic algorithm. Then they improved a hybrid stochastic/deterministic optimization approach developed based on a combination of genetic algorithm and simulated annealing (GA+SA) to minimize either the cost of the system product (fresh water) and/or maximizing the exergetic efficiency of the multi-effects distillation (MED) desalination systems with thermo-vapor compressor (TVC) [24]. The results showed that the hybrid SA-GA method is able to obtain a better solution faster than a conventional genetic algorithm. Shakib et al. [25] developed a comprehensive thermodynamic model for METVC in the paper. The main objective of the paper is optimization of MED desalination with thermal vapor compression (METVC) from economical and thermodynamic point of view. Four objective functions are chosen as four cases for optimization, including minimizing specific heat transfer area, maximizing exergy efficiency, maximizing performance ratio (PR), and minimizing specific heat transfer area and maximizing PR. It can be seen that the results of multi-objective problem are perfect and more reasonable than other cases.

Although the research on the multi-effect evaporation system design has made great progress, studies on the multi-objective optimization of PF-MEE systems to maximize gain output ratio (GOR) and minimize simplified cost of water (SCOW), simultaneously, are scarce. To our knowledge, when designing a PF-MEE system, GOR as a key parameter measuring the system performance and the unit costs of the system (SCOW) should be considered simultaneously. Finding a compromise between them is important. In this paper, to maximize gain output ratio (GOR) and minimize simplified cost of water (SCOW), the effect of input variables, such as the number of the effect (n), the top brine temperature (T_b), the apparent temperature difference (Δt) and the recovery ratio (RR_1) are studied using the multi-objective genetic algorithm. The purpose of the research is to find the optimal design scheme to meet the different requirements.

2. Materials and methods

2.1. Multi-objective genetic algorithm

Genetic algorithm (GA) is a computational model of biological evolution that simulates the natural selection and genetic mechanism of Darwinian biological evolution

[26]. It is a class of parallel, iterative, and population-based search to find the optimal solution in a large solution domain by simulating the natural evolution process [20,27,28]. A genetic algorithm starts with a population that represents a possible potential solution, while a population consists of a collection of chromosomes. One or more features of each chromosome are controlled by each gene. After the original population is generated, according to the principle of survival of the fittest and the evolution, each subsequent generation evolution produces better approximate solutions. In each generation, according to the size of fitness, the chromosomes are selected for the transition [29]. Utilizing natural genetics, crossover and mutation take place for producing on behalf of the new solution set of the population.

In the case of multi-objective problems, different from the single-objective optimization question, in most cases, no unique optimal solution could be achieved, and a set of solutions can be obtained by searching following the concept of Pareto optimality [20]. When several conflicting objective functions exist, a set of solutions called the Pareto front can provide the best possible compromises between the objectives. By the definition of the Pareto-optimality, no other solution could exist in the feasible range that is at least as good as some member of the Pareto set, in terms of all the objectives, and strictly betters in terms of at least one [20]. Pareto set can provide a range of useful options to the decision-maker, who can then choose the right solution (operation point) according to requirements and preferences.

2.2. Process description

Fig. 1 shows the parallel-feed configuration of the MEE system. In the parallel-feed MEE system, brine is distributed almost equally to each effect. Different from the conventional parallel-feed MEE system, it adds the preheating process before the feed seawater flowing to each evaporator. Part of the secondary steam from the first effect exchanges heats with the brine in the preheater, which will increase the temperature of the brine. This process can decrease the temperature difference between the feed seawater outside the tubes and the steam inside the tubes and improve the gain output ratio (GOR) of the system.

2.3. Mathematical model

To simplify the model calculation, some assumptions have been considered:

- Steady-state operation [30].
- The temperature difference has been assumed to be 1°C as a real design value between the brine and the vapor in one evaporator, which includes BPE, non-equilibrium allowance (NEA), and the thermodynamic losses [31].
- Isothermal physical properties have been considered for all cases [32].
- The temperature difference between all effects and between the preheaters is assumed to be the same.
- The heat transfer area of each evaporator is assumed to be the same [7].
- Seawater salinity and seawater temperature are assumed to be 35,000 ppm and 25°C, respectively.

2.3.1. First effect

Fig. 2 demonstrates a flow diagram of the first effect for the parallel-feed MEE system.

Mass balance:

In the parallel-feed MEE system, feed water is distributed almost equally to each effect.

$$M_{f,1} = M_{f,2} = \ldots\ldots = M_{f,i} = M_{f,n} = \frac{M_{f,t}}{n} \tag{1}$$

$$M_{f,1} = M_{v,1} + M_{b,1} \tag{2}$$

Salt balance:

$$M_{f,1} X_{\text{in},1} = M_{b,1} + X_{\text{out},1} \tag{3}$$

Energy balance:

$$M_{s,1}\lambda_s\left(\psi_{\text{in},1} - \psi_{\text{out},1}\right) = M_{v,1}\lambda_v + M_{f,1}\left(T_{b,1} - T_{f,1}\right)C_p \tag{4}$$

where ψ is the vapor quantity of the steam.

In the first effect, the steam in the tube is considered to condense completely. $\Psi_{\text{in},1}$ and $\psi_{\text{out},1}$ shall be 1 and 0, respectively.

Heat transfer equation of evaporator:

$$Q_{E,1} = M_{s,1}\lambda_s\left(\psi_{\text{in},1} - \psi_{\text{out},1}\right) = h_{e,1}\left(\text{LMTD}_{e,1}\right)A_{E,1} \tag{5}$$

The overall heat transfer coefficient is calculated using the following correlation [7]:

$$h_e = 1{,}961.9 + 12.6T_b - 9.6 \times 10^{-2}T_b^2 + 3.16 \times 10^{-4}T_b^3 \tag{6}$$

The log mean temperature difference ($\text{LMTD}_{e,1}$) is calculated according to Eq. (7).

$$\text{LMTD}_{e,1} = \frac{T_{b,1} - T_{f,1}}{\ln\left(\dfrac{T_{s,1} - T_{f,1}}{T_{s,1} - T_{b,1}}\right)} \tag{7}$$

Heat transfer equation of preheater:

$$\Phi_1 = \frac{M_{f,1}\left(T_{o,1} - T_{i,1}\right)C_p}{M_{v,1}\lambda_v} \tag{8}$$

$$A_{\text{ph},1} = \frac{M_{f,1}\left(T_{o,1} - T_{i,1}\right)C_p}{h_{p,1}\left(\text{LMTD}_{\text{ph},1}\right)} \tag{9}$$

where Φ is a mass fraction of vapor condensation in the preheater, $h_{p,1}$ is the heat transfer coefficient calculated by Eq. (10).

$$h_p = 1{,}719.4 + 3.2063T_b - 1.5971 \times 10^{-2}T_b^2 - 1.9918 \times 10^{-4}T_b^3 \tag{10}$$

$$\text{LMTD}_{\text{ph},1} = \frac{T_{o,1} - T_{i,1}}{\ln\left(\dfrac{T_{v,1} - T_{i,1}}{T_{v,1} - T_{o,1}}\right)} \tag{11}$$
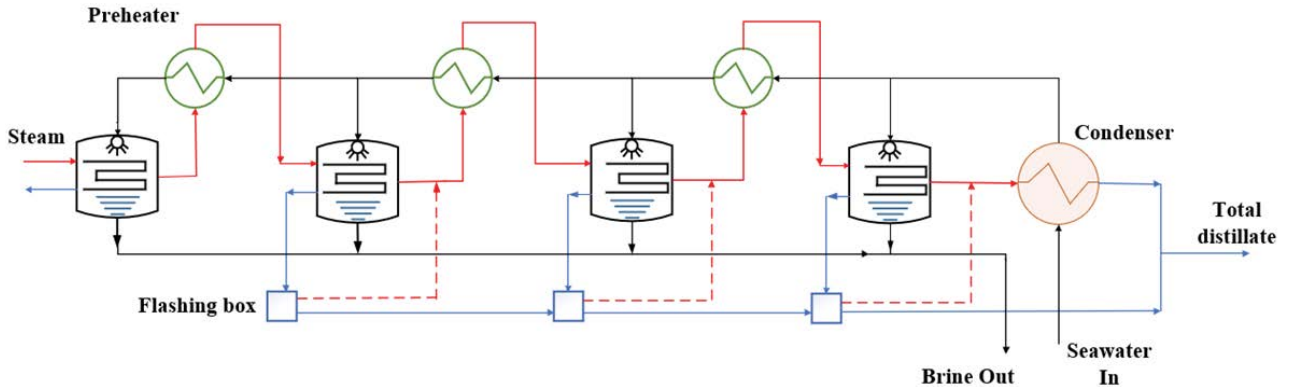
Fig. 1. Schematic of the parallel-feed MEE configuration for *n* number of effects.
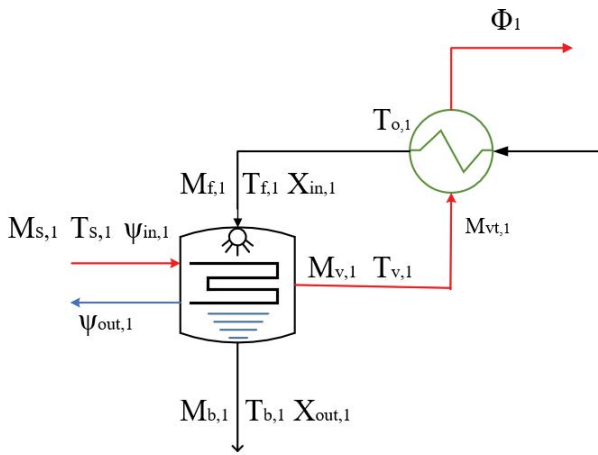
Fig. 2. Flow diagram of the first effect for parallel-feed MEE system.

Fig. 3. Flow diagram of the *i*th effect for parallel-feed MEE system.

2.3.2. ith effect

For improving the performance of the MEE system, a series of flashing boxes are necessary, which receives distillate from the previous flashing box (except that of the second effect) and the current evaporator (Fig. 3). The mass flow rate of steam produced by flash in flashing box is denoted by $M_{fv,i}$ and is mixed with the vapor produced ($M_{v,i}$) in the evaporator, which is redirected to the preheater. Therefore, we have

$$M_{fv,i}\lambda_v = \left(M_{v,i-1} + M_{fb,i-1}\right)C_p\left(T_{v,i-1} - T_{v,i} - \text{NEA}\right) \quad (12)$$

$$M_{vt,i} = M_{v,i} + M_{fv,i} \quad (13)$$

$$M_{fb,i} = M_{v,i-1} + M_{fb,i-1} - M_{fv,i} \quad (14)$$

where NEA is the non-equilibrium allowance that is a measure for the efficiency of the flashing process can be calculated according to the following equation:

$$\text{NEA} = \frac{33\left(T_{v,i-1} - T_v\right)^{0.55}}{T_v} \quad (15)$$

Heat transfer equation of preheater:

$$\Phi_i = \frac{\left(M_{f,1} + M_{f,2} + \ldots + M_{f,i}\right)\left(T_{o,i} - T_{i,i}\right)C_p}{M_{vt,i}\lambda_v} \quad (16)$$

$$A_{ph,i} = \frac{\left(M_{f,1} + M_{f,2} + \ldots + M_{f,i}\right)\left(T_{o,i} - T_{i,i}\right)C_p}{h_{p,i}\left(\text{LMTD}_{ph,i}\right)} \quad (17)$$

2.3.3. Last effect

In the last effect, to condense all the steam into the water, the heat transfer area must be large enough and the cooling seawater should be sufficient (Fig. 4).

Heat transfer equation of condenser:

$$M_{sw} = \frac{M_{vt,n}\lambda_v}{\left(T_{cw,out} - T_{cw,in}\right)C_p} \quad (18)$$

$$A_{ph,n} = \frac{M_{vt,n}\lambda_v}{h_{p,n}\left(\text{LMTD}_{c,n}\right)} \quad (19)$$

The mass flow rate of total distillate is calculated as follows:

$$M_d = M_{fb,n} + M_{vt,n} \tag{20}$$

2.4. Performance index

Gain output ratio (GOR) is the most important index to measure the system performance of an MEE system and it can be calculated as follows:

$$GOR = \frac{M_d}{M_s} \tag{21}$$

Recovery ratio (RR), which is the feed flow rate supplied to the ratio of the distillate product flow rate, is obtained as follows [31]:

$$RR = \frac{M_f}{M_b} \tag{22}$$

For the parallel-feed MEE, the recovery ratio of each effect decreases along the steam flowing direction. The recovery ratio of the first effect is a key factor to affect system performance. In this paper, the recovery ratio of the first effect is defined as an input variable of the objective function, which is expressed as follows:

$$RR_1 = \frac{M_{f,1}}{M_{b,1}} \tag{23}$$

2.5. Economical indicator

In desalination, similarly, with other industries, the cost of the final product is one of the most important criteria that define the commercial success of a specific technology [33].

MEE plants involve several kinds of costs and revenues over a long period during the operation life, including initial capital cost, running cost, labor and chemical cost, etc. In the paper [34], a parameter called Simplified Cost of Water (SCOW) is used to define the initial capital cost, which can be calculated using Eq. (24).

$$SCOW = \frac{(I_0 \varphi) + C_t}{M_d} \tag{24}$$

where i is the interest rate and n is the number of years of the economic life of the system, taken as 0.05 and 20, respectively [34]. By calculation, ϕ is 0.85.

In Eq. (24), it is assumed that every year (from year 1 to year n), the desalination plant produces the same amount of water (M_d) and has the same running cost (C_t).

Capital cost (I_0) contains several factors, such as equipment, materials, pumps, cost of land, initial design and permitting, and so on. However, the main purpose of economic analysis is to assess the impact of any proposed design options on the final cost of water. For simplifying the calculation, the correlations for estimating the specific capital cost of multi-effect distillation plants considering is proposed by the study of Yilmaz and Söylemez [30]:

$$C_{MED} = 6,291 M_d^{-0.135} \left[(1 - f_{HEX}) + f_{HEX} \left(\frac{HEX_{area}}{HEX_{area,ref}} \right)^{0.8} \right] \tag{25}$$

where f_{HEX} is the cost fraction of the evaporator, and the constant of 0.8 is used to take into consideration the plant capacity, M_d is the distillate flow rate, HEX_{area} is the heat exchanger area including evaporators and preheaters, $HEX_{area,ref}$, which is the HEX_{area} of the reference plant, is considered to be 8,841 m². C_{MED} is given in \$/(m³/d). The capital cost (I_0) in \$ is calculated as follows:

$$I_0 = \frac{C_{MED} M_d}{R} \tag{26}$$

where R is the fraction of the capital cost that corresponds to the evaporator that is considered to be 40% [35].

Running cost (C_t) is the annual operating cost, which mainly includes the cost of energy (heat and electricity), seawater pretreatment chemical, labor, maintenance, and management, which can be calculated according to Eq. (27).

$$C_t = C_{st} + C_{el} + C_{sp} + C_{os} + C_{mt} + C_{mg} \tag{27}$$

The detailed compositions of the running cost are shown in Table 1.

2.6. Expression and approximation of the objective functions

In this paper, gain output ratio (GOR) and simplified cost of water (SCOW) are considered as two objective functions and the number of the effect (n), the top brine temperature (T_b), the apparent temperature difference (Δt), and the recovery ratio of the first effect (RR_1) are defined as the input variables. The objective functions can be described mathematically by:

$$\text{Objective function}: \begin{cases} \max GOR = f_1(n, T_b, \Delta t, RR_1) \\ \min SCOW = f_2(n, T_b, \Delta t, RR_1) \end{cases} \tag{28}$$

$$\text{Constraint conditions}: \begin{cases} 3 \le n \le 14 \\ 0°C < T_b \le 80°C \\ 2°C \le \Delta t \le 4°C \\ 2 \le RR_1 \le 4 \\ T_b - (\Delta t + 1)(n - 1) > 35°C \end{cases} \tag{29}$$

A computing program is necessary to solve the multi-objective optimization problem. A non-dominated sorting-based multi-objective evolutionary algorithm, called non-dominated sorting genetic algorithm-II (NSGA-II) has been developed in Python language [38].

The main parameters used in the program are set to the following values:

- Using crowding distance sorting
- Selection function: tournament selection
- Crossover operator: uniform
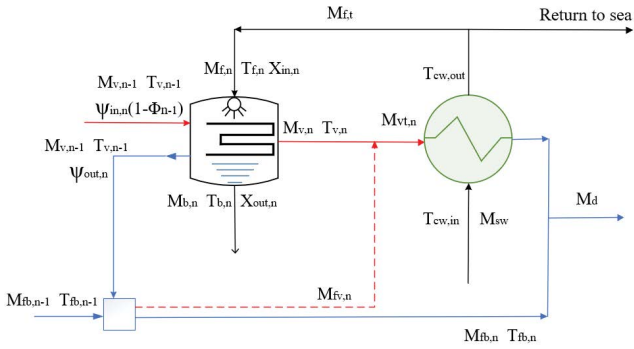
Fig. 4. Flow diagram of the last effect for parallel-feed MEE system.

- Crossover fraction: 1
- Population size: 200
- Maximum number of the iteration: 1000

However, the MEE system is a complex system that the relation of the function of each effect is nonlinear. It is difficult to find the function relation between the two objective functions and the input variables. It is necessary to make some reasonable assumptions and approximate the objective functions.

The assumptions are listed below:

- The inlet and outlet temperature of each evaporator and preheater should be first defined (Fig. 5), which can be expressed by the top brine temperature.

In each evaporator:

$$T_{b,n} = T_{b,1} - (n-1)\Delta T \tag{30}$$

$$T_{v,n} = T_{b,n} + \Delta t \tag{31}$$

$$T_{f,n} = T_{b,n} - \Delta t \tag{32}$$
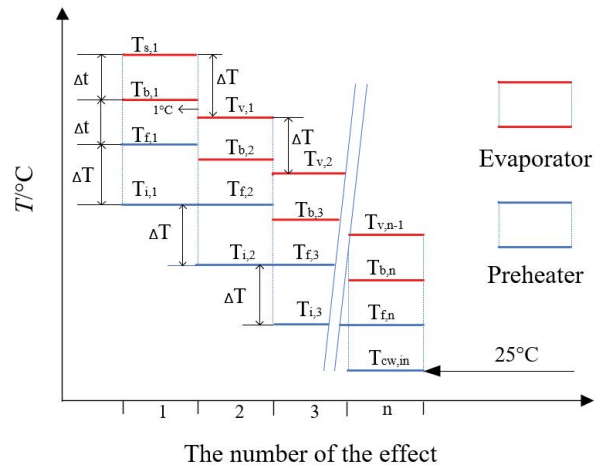
Fig. 5. Temperature flow chart of the MEE system.

In each preheater:

$$T_{i,n} = T_{f,n} - \Delta T \tag{33}$$

where ΔT is the temperature difference between each evaporator and the preheater, Δt is the apparent temperature difference of the evaporator, $\Delta T = \Delta t + 1$.

- When calculation, some parameters with the brine temperature as the independent variable, such as heat transfer coefficient, special heat, the latent heat of evaporation, the non-equilibrium allowance (NEA), etc., the value of the temperature is the mean brine temperature, which can be expressed by:

$$T_{b,\text{mean}} = \frac{2T_{b,1} - (n-1)\Delta T}{2} \tag{34}$$

Table 1
Compositions of the running cost

Parameters	Symbol	Equation	Description	Ref.
Steam	C_{st}	$C_{st} = M_s \times P_{st}$	P_{st} is the steam price 2 \$/ton	[32,33]
Electricity	C_{el}	$C_{el} = 365 \times 24 \times P_{el} \times Z_{pump} \times M_{sw}$	P_{el} is unit electricity price 0.07 \$/kWh, Z_{pump} is the sum of pump power consumption in kWh/m³	[36]
			$2 \leq m_{\text{water}} \leq 32 \quad 100 \leq \Delta p \leq 6{,}200$	[37]
	Z_{pump}	$Z_{pump} = 13.92\, m_{\text{water}}\, \Delta p^{0.55} e^{1.05}$	$1.8 \leq e \leq 9 \quad e = \dfrac{\eta_{pump}}{1 - \eta_{pump}}$	
Seawater pretreatment	C_{sp}	$C_{sp} = M_{ft} m_{cc} P_c$	m_{cc} is chemical consumption per ton seawater 0.005 kg/ton, P_c is the unit chemical cost 1.46 \$/kg	[36]
Operators' salary	C_{os}	$C_{os} = 6{,}000 \times 6$	Yearly operators' salary is 6,000 \$/operator with the plant using six operating workers	[36]
Maintenance cost	C_{mt}	$C_{mt} = 1.5\% \times I_0$	Annual maintenance cost is estimated as 1.5% of the capital cost	[36]
Management cost	C_{mg}	$C_{mg} = 20\% \times C_{os}$	Annual management cost is estimated as 20% of the labor cost	[36]

- The design of the evaporator adopts the equal area design approach, that is, the heat transfer area of other effects equals that of the first one.
- The brine temperature of the last effect is above 35°C.

The main approximation of the function expressions is about the accumulated vapor of each effect. The mass flow of accumulated vapor of each effect is approximated by a decreasing arithmetic progression (Table 2).

According to Table 2, the formula of the general term of the arithmetic progression is expressed by:

$$M_{v,n} = M_{s,1} - \frac{M_f C_p \Delta t}{n\lambda} - \frac{n(n-1)}{2} \frac{M_f C_p (\Delta t + 1)}{n\lambda}$$
$$- (n-1) \frac{M_f C_p \Delta t}{n\lambda} + \frac{n(n-1)}{2} \frac{M_{v,1} C_p (\Delta t - NEA)}{\lambda} \quad (35)$$

The sum of the first *n* terms of the arithmetic progression (total distillation production) is calculated by:

$$M_d = nM_{s,1} - n\frac{M_f C_p \Delta t}{n\lambda} - \frac{n(n^2-1)}{6} \frac{M_f C_p (\Delta t + 1)}{n\lambda}$$
$$- \frac{n(n-1)}{2} \frac{M_f C_p \Delta t}{n\lambda} + \frac{n(n^2-1)}{6} \frac{M_{v,1} C_p (\Delta t - NEA)}{\lambda} \quad (36)$$

3. Results and discussion

3.1. Accuracy analysis on the approximation function

In the previous section, the approximation functions on the accumulated vapor of each effect were mentioned. For verifying the accuracy of the approximation function, comparisons of three case studies with different input parameters (Table 3) between the theoretical and the approximation value should be discussed.

Figs. 6–8 demonstrate the comparisons of the accumulated vapor of each effect between theoretical value and approximation value for three cases. The results show that the approximation value of accumulated vapor fits well with the theoretical one with a small difference of below 4%. For the whole system, the differences in the total distillate production and GOR became smaller (Table 4). The main reason that the approximation function has a small error is ignoring the impact of the flashing on the whole system. Generally, flashing vapor in the flashing box takes a very minor part of the total distillate production about below 2%. It assumes that the mass flow rate entering each flashing box shows a linear relation is reasonable. So it follows that the approximation function is accurate that can be used in the MEE system optimation and estimation.

3.2. Study on the function values and variables

To solve the optimization problem, except for the parameters mentioned above another one (heating steam mass flow rate or the total distillate production) needs to be also defined. Under the condition of $M_s = 3,000$ kg/h, a series of Pareto points, which are demonstrated in Fig. 9, forms Pareto optimal solutions. The value of the SCOW and GOR has the same trend, that is, with the GOR increase, the value of the SCOW becomes bigger. Therefore, finding a point with the smallest SCOW and the biggest GOR is contradictory. Although the Pareto set can provide a range of useful options to the decision-maker, after comprehensive considering the best design point can be selected among the Pareto optimal solutions. As shown in Fig. 9, point A and point B are both ends of the curve with the minimum and the maximum value, which are called the optimal yield point and optimal economical point, respectively. Just for the sake of minimum SCOW and maximum GOR, point A and point B may be the best choices.

The purpose of multi-objective optimization is to seek the optimal design variables to satisfy the constraint requirement of objective functions. The effect of the variables

Table 2
Function expressions of accumulated vapor of each effect

Symbol	Theoretical value	Approximation
$M_{v,1}$	$M_{s,1} - \dfrac{M_f C_p \Delta t}{n\lambda}$	$M_{s,1} - \dfrac{M_f C_p \Delta t}{n\lambda}$
$M_{v,2}$	$M_{v,1} - \dfrac{M_f C_p (\Delta t + 1)}{n\lambda} - \dfrac{M_f C_p \Delta t}{n\lambda} + \dfrac{M_{v,1} C_p (\Delta t - NEA)}{\lambda}$	$M_{v,1} - \dfrac{M_f C_p (\Delta t + 1)}{n\lambda} - \dfrac{M_f C_p \Delta t}{n\lambda} + \dfrac{M_{v,1} C_p (\Delta t - NEA)}{\lambda}$
$M_{v,3}$	$M_{v,2} - \dfrac{2M_f C_p (\Delta t + 1)}{n\lambda} - \dfrac{M_f C_p \Delta t}{n\lambda} + \dfrac{(M_{v,1} + M_{v,2} - M_{fv,1}) C_p (\Delta t - NEA)}{\lambda}$	$M_{v,2} - \dfrac{2M_f C_p (\Delta t + 1)}{n\lambda} - \dfrac{M_f C_p \Delta t}{n\lambda} + \dfrac{2M_{v,1} C_p (\Delta t - NEA)}{\lambda}$
……	……	……
$M_{v,n}$	$M_{v,n-1} - \dfrac{(n-1)M_f C_p (\Delta t + 1)}{n\lambda} - \dfrac{M_f C_p \Delta t}{n\lambda} + \dfrac{\left(\sum_1^{n-1} M_{v,i} - \sum_1^{n-2} M_{fv,i}\right) C_p (\Delta t - NEA)}{\lambda}$	$M_{v,n-1} - \dfrac{(n-1)M_f C_p (\Delta t + 1)}{n\lambda} - \dfrac{M_f C_p \Delta t}{n\lambda} + \dfrac{(n-1)M_{v,1} C_p (\Delta t - NEA)}{\lambda}$
Conclusion	Irregularity	Arithmetic progression

Table 3
Input parameters of three cases

Parameters		Case 1	Case 2	Case 3
Feedwater mass flow rate, kg/h	$M_{f,t}$	1,000	5,000	10,000
Heating steam mass flow rate, kg/h	$M_{s,1}$	100	300	500
Top brine temperature, °C	$T_{b,1}$	60	70	80
Apparent temperature difference, °C	Δt	3	2.5	2
Number of effects	n	8	10	14
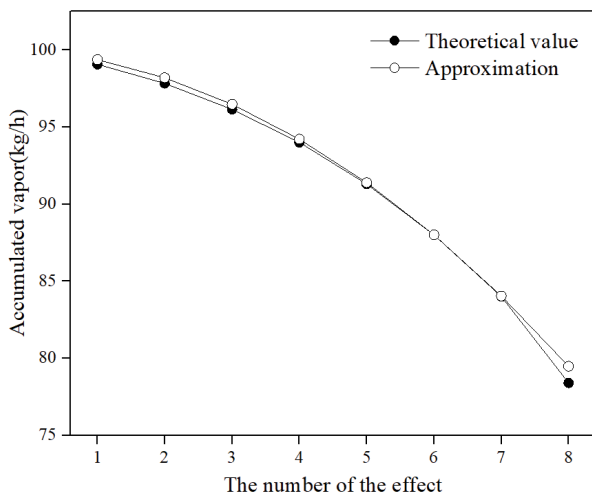
Fig. 6. Accumulated vapor of each effect for Case 1.
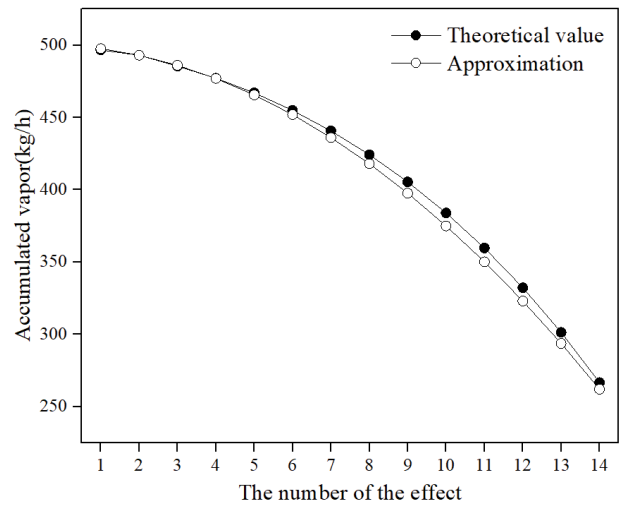
Fig. 8. Accumulated vapor of each effect for Case 3.
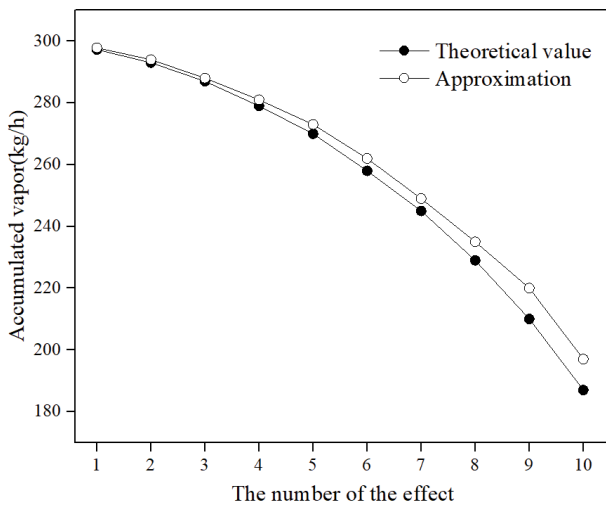
Fig. 7. Accumulated vapor of each effect for Case 2.
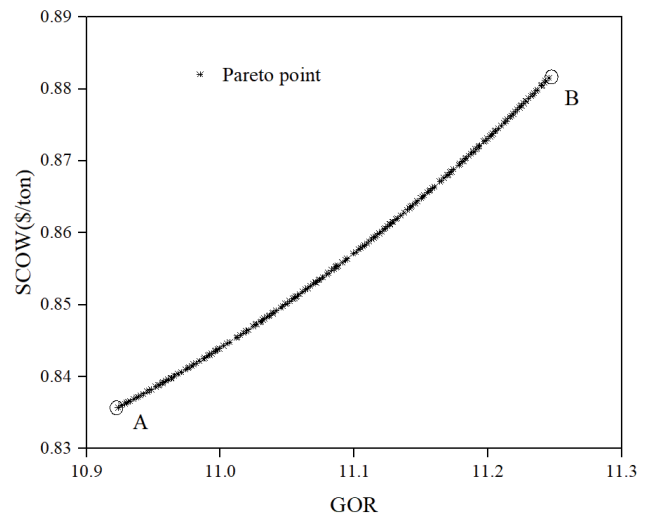
Fig. 9. Pareto optimal solutions for SCOW and GOR for $n = 14$.

on the values of objective functions is necessary to research. There are four variables, namely, the number of the effect (n), the top brine temperature (T_b), the apparent temperature difference (Δt), and the recovery ratio of the first effect (RR_1). Under the different number of the effect conditions, the other three variables are studied in 3D plots (Fig. 10). As shown in Fig. 10, the value of the variable Δt is scattered

over the whole simulation range, whereas the top brine temperature (T_b) and Recovery ratio (RR_1) are not. Whatever the other variables vary, the top brine temperature (T_b) and recovery ratio (RR_1) are always the upper limits of the simulation interval, which are 80°C and 4, respectively. It is found that, under the same other design conditions, the greater top brine temperature and the bigger recovery ratio will lead GOR to become bigger and SCOW smaller.

Table 4
Total distillate production and GOR of the theoretical value and the approximation

Parameters		Case 1	Case 2	Case 3
Total distillate production (M_d), kg/h	Theoretical value	728	2,555	5,788
	Approximation value	731	2,596	5,726
	Error	0.4%	1.6%	1.0%
Gain output ratio, GOR	Theoretical value	7.28	8.51	11.57
	Approximation value	7.31	8.65	11.45
	Error	0.3%	1.6%	1.0%
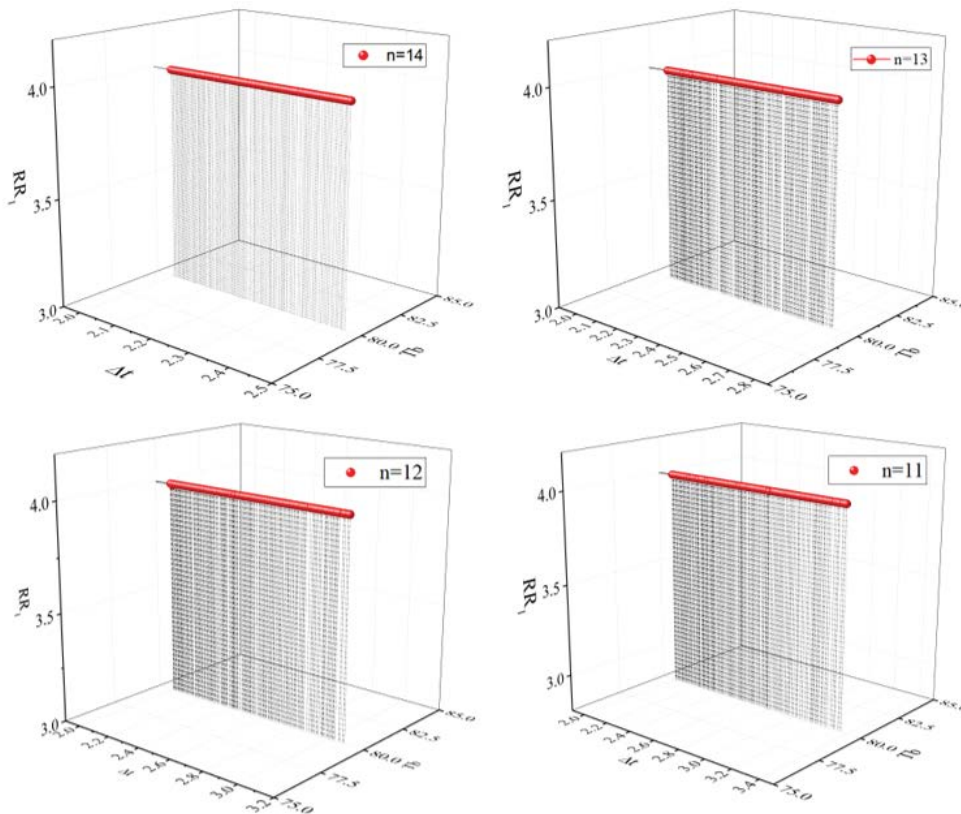
Fig. 10. Variables of T_t, n and Δt for n = 11, 12, 13, 14.

3.3. Case study

According to various user requirements and usage scenarios, generally, there are two different approaches when designing the MEE system.

- Define the steam flow rate (DS). In some places already with sufficient steam such as the thermal power plant, boiler factory, or other factories, using the original steam as the heat source to design an MEE system can not only reuse the steam to reduce the energy waste but also produce more benefits.
- Define the total distillate production (DTD). In some dry and thirsty places, the yield of an MEE plant is the first consideration for decision-makers. And then steam generators are constructed to satisfy the heat source need of the system.

The effectiveness of the two approaches using multi-objective optimization is assessed by analyzing the two cases.

3.3.1. Case 1

Data for case 1 are taken from Darwish and Abdulrahim [10], which is based on a conventional parallel-feed MEE system without preheaters. In this paper, a parallel-feed configuration with a series of the preheaters was introduced. The comparisons between the data from [10] and the calculation results with the novel configuration are listed in Table 5. As shown in Table 5, under almost the same input parameters, the total distillate production and GOR of the parallel-feed MEE with a series of preheaters have improved comparing the conventional one about the relative error of 7%. It indicates that the novel parallel-feed

configuration is better than the conventional one on the system performance.

Moreover, using multi-objective optimization to optimize the calculation results can further improve the performance. The optimized results are listed in Table 6. For the DS design approach, the heating steam mass flow from the calculation results of the novel configuration (Original plan) is defined as the input variable. GOR of the optimal yield solution is greater than that of the original plan about 10%, but there is no advantage in SCOW. Comparing the optimal yield solution, the optimal economical solution has a smaller GOR and SCOW that is still better than the original plan with an 8% increase on GOR and a 5% decrease on SCOW. For the DTD design approach, the input variable total distillate production (M_d) is equal to that of the original plan. A similar phenomenon as the DS design approach appears that the optimal economical

solution is the most appropriate. In case 1, it seems that the two optimal economical solutions may be suitable plans. However, the minor differences between the two design approach, DS and DTD, need to be discussed.

As shown in Fig. 11, the curves of Pareto optimal solutions for SCOW and GOR of DS and DTD design approaches have the same trend except that the value of SCOW of the DTD design approach is smaller than that of DS about a range of 3%–3.8%. That is because at the same GOR condition DTD design approach leads to less heating steam input that is an important part of the running cost. Although SCOW of the DS design approach is higher, there is an advantage not to be neglected that is the more total distillate production. For the optimized results of case 1, the optimal economical solution of DS has the more total distillate production, the optimal economical solution of DTD has the less heating steam input and cost.

Table 5
Comparisons between the data from the study of Darwish and Abdulrahim [10] and the calculation results

Parameters	Darwish and Abdulrahim [10]	Calculation results (Original plan)
Feed water mass flow rate, kg/s, M_f	157.85	157.85
Heating steam mass flow rate, kg/s, M_s	15.778	15.778
Feedwater temperature, °C, T_f	73.3	73
Top brine temperature, °C, $T_{b,1}$	64	64
Brine temperature of the 2nd effect, °C, $T_{b,2}$	54.7	55
Brine temperature of the 3rd effect, °C, $T_{b,3}$	45.3	45
Brine temperature of the 4th effect, °C, $T_{b,4}$	36	36
Number of the effect	4	4
Total distillate production, kg/s, M_d	52.616	56.38
GOR	3.33	3.57
SCOW, $/ton	Unknown	1.8

Table 6
Optimized results for Case 1

Design approach	DS		DTD	
Input variables	M_s = 15.78 kg/s n = 4 0°C < T_b ≤ 64°C 2°C ≤ Δt ≤ 4°C 2 ≤ RR_1 ≤ 4		M_d = 56.38 kg/s n = 4 0°C < T_b ≤ 64°C 2°C ≤ Δt ≤ 4°C 2 ≤ RR_1 ≤ 4	
Get results	Optimal yield	Optimal economical	Optimal yield	Optimal economical
GOR	3.9	3.85	3.9	3.85
SCOW, $/ton	1.99	1.72	1.92	1.67
M_s, kg/s	15.78	15.78	14.46	14.64
M_f, kg/s	83.78	83.44	76.77	77.42
n	4	4	4	4
T_b, °C	64	64	64	64
Δt, °C	2	3.78	2	3.74
RR_1	4	4	4	4
M_d, kg/s	61.54	60.75	56.38	56.38
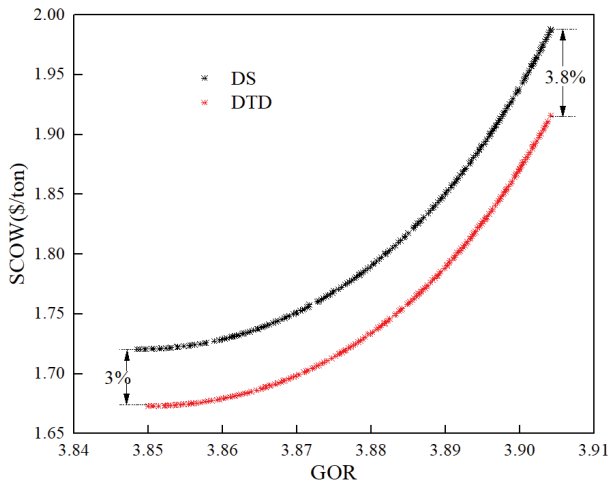
Fig. 11. Pareto optimal solutions for SCOW and GOR of DS and DTD design approaches.

3.3.2. Case 2

Case 2 is used to simulate a real design scenario. A factory wants to build up an MEE plant, which can provide industrial steam with a mass flow rate of not more than 0.5 kg/s and with a temperature of 80°C. The requirement is that the total distillate production should not be less than 4.8 kg/s and the unit cost of water per ton should not be more than 0.8 $/ton. According to the existing conditions and the proposed requirements, a series of design plans are presented to decision-makers to choose from.

The main design steps are listed below:

- Define the input parameters.
- Using DS and DTD design approaches to optimize the plan.
- Select the solution that meets the requirements.
- Calculate other design parameters.
  Input parameters are listed in Table 7.

Two design approaches are used to optimize the design plans. For the DS design approach, the input parameter heating steam mass flow is 0.5 kg/s, the constraint conditions are $M_d \geq 4.8$ kg/s, SCOW ≤ 0.8 $/ton. Pareto optimal solutions for SCOW and GOR of DS design approach for n = 10, 11, 12, 13 is demonstrated in Fig. 12. Two dotted lines GOR = 9.6 and SCOW = 0.8 form a region where exists a solution set that satisfies the constraints. Outside of Zone 1, Pareto optimal solutions for n = 10 and 11 are invalid. Part of the curves of Pareto optimal solutions of n = 12, 13 locate in Zone 1 and intersect the dotted line at points 2 and 4 that are optimal yield points. Points 1 and 3 are optimal economical points where SCOW is minimum for n = 12 and 13, respectively. Four points (1–4) are chosen as the optimal solutions in the DS design approach. For another design approach DTD, the parameter total distillate production is defined as 4.8 kg/s, the constraint conditions are $M_s \leq 0.5$ kg/s, SCOW ≤ 0.8 $/ton. Fig. 13 demonstrates a similar phenomenon to the DS design approach. A total of eight points 1–4, A - D are selected as alternative options for further discussion.

Table 7
Input parameters and requirements for case 2

Number of effects (n)	3–13
Heating steam mass flow (M_s)	0.5 kg/s
Heating steam temperature (T_s)	80°C
Total distillate production (M_d)	4.8 kg/s [5]
Unit cost of water per ton (SCOW)	≤0.8 $/ton
Feedwater temperature ($T_{cw,in}$)	25°C
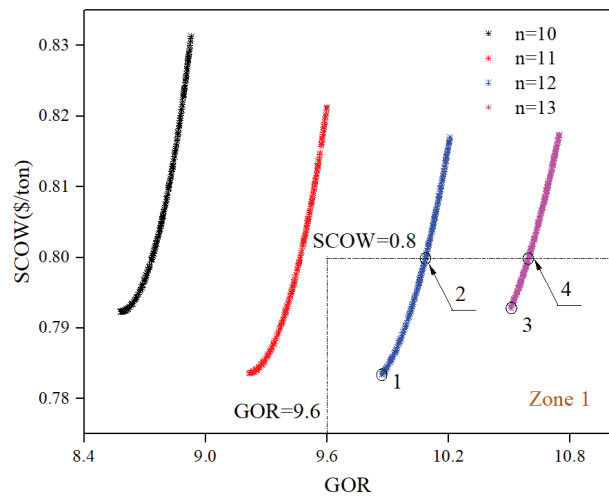
Fig. 12. Pareto optimal solutions for SCOW and GOR of DS design approach for n = 10, 11, 12, 13.

The detailed calculation results of eight plans are listed in Table 8. For the DS design approach, among the four plans (1–4), 2 and 3 are excluded due to GOR of them are not maximum and SCOW not minimum. Because of the same reason, plans B and C are not selected as the final decision in the DTD design approach. In the end, four scenarios (black stars in Table 8) with their advantages are present to the decision-makers (Table 9), who can select the most appropriate one according to their preferences.

4. Conclusions

The paper is focused on the design optimization of the parallel-feeding multi-effect evaporation using a multi-objective genetic algorithm. Gain output ratio (GOR) and simplified cost of water (SCOW) are considered as two objective functions and the number of the effect (n), the top brine temperature (T_b), the apparent temperature difference (Δt), and the recovery ratio of the first effect (RR_1) are defined as the input variables.

First, the model is based on the parallel-feeding configuration with a series of preheaters. To facilitate multi-objective optimization, the complicated mathematic model is approximated and verified. The results show that the approximate function has a minor error to calculate the accumulated vapor of each effect.

Second, comparisons of performance between the parallel-feeding configuration with and without preheaters

Table 8
Optimized results for Case 2

Design approach	DS				DTD			
Number of effects	12		13		12		13	
	O-Y	O-E	O-Y	O-E	O-Y	O-E	O-Y	O-E
Point	2	1	4	3	B	A	D	C
n	12	12	13	13	12	12	13	13
GOR	10	9.8	10.6	10.5	10.09	9.87	10.61	10.5
SCOW, \$/ton	0.8	0.78	0.8	0.79	0.8	0.78	0.8	0.792
M_s, kg/s	0.5	0.5	0.5	0.5	0.476	0.486	0.452	0.457
M_f, kg/s	7.96	7.95	8.62	8.61	7.58	7.58	7.79	7.88
M_d, kg/s	5	4.9	5.3	5.25	4.8	4.8	4.8	4.8
T_b, °C	76	76	76	76	76	76	76	76
Δt, °C	2.3	2.7	2.3	2.3	2.26	2.72	2.23	2.42
RR_1	4	4	4	4	4	4	4	4
$A_{E,total}$	2,423	2,064	2,625	2,620	2,348	2,348	2,448	2,280
$A_{ph,total}$	123	112	145	140	118	118	134	128
A_c	104	176	111	109	94	94	91	122
Decision		*	*			*	*	

O-Y: Optimal yield; O-E: optimal economical.

Table 9
Advantage of final selected four scenarios

Scenario	Advantage
1	More total distillate production, smaller SCOW
4	More distillate production, bigger GOR
A	Less heating steam consumption, smaller SCOW
D	Less heating steam consumption, bigger GOR

are presented. It indicates that GOR of the parallel-feed configuration with preheater is better than that without preheater that is from the previous literature about 7%. The calculation results can be further optimized to increase GOR by about 8% and to decrease SCOW by 5% using a multi-objective genetic algorithm.

Third, the effect of the input variables, the number of the effect (n), the top brine temperature (T_b), the apparent temperature difference (Δt), and the recovery ratio of the first effect (RR_1) on GOR and SCOW is studied. Whatever the other variables vary, the top brine temperature (T_b) and recovery ratio (RR_1) are always the upper limits of the simulation interval, which are 80°C and 4, respectively. It is found that under the same other design conditions, the greater top brine temperature and the bigger recovery ratio will lead GOR to become bigger and SCOW smaller.

Fourth, a case study is performed to simulate a real design scenario. Two design approaches, DS and DTD and two evaluation criteria, optimal yield and optimal economical, are proposed. Through comparison and selection, four final proposals with their advantages are selected and presented to the decision-makers.

In the end, the MEE system design is a complex task and affected by a series of variables. The present study has
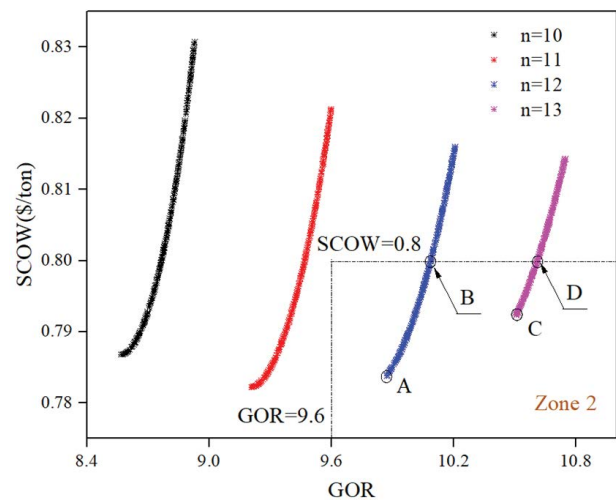
Fig. 13. Pareto optimal solutions for SCOW and GOR of DTD design approach for n = 10, 11, 12, 13.

demonstrated the successful application of a multi-objective genetic algorithm for the optimal design of parallel-feeding configuration.

Symbols

M_f	—	Mass flow rate of feed water, kg/s
M_s	—	Mass flow rate of heating steam, kg/s
M_b	—	Mass flow rate of brine, kg/s
M_v	—	Mass flow rate of vapor, kg/s
M_{sw}	—	Mass flow rate of seawater, kg/s
M_{fv}	—	Mass flow rate of the vapor generated in the freshwater flashing box, kg/s

M_{vt}	—	Total mass flow rate of the vapor entering the preheater, kg/s
M_{fb}	—	Mass flow rate of the remaining freshwater leaving the freshwater flashing box, kg/s
M_d	—	Mass flow rate of total distillate, kg/s
X	—	Salinity of brine, g/kg
ψ	—	Vapor quantity of the steam,
T_s	—	Steam temperature, °C
T_f	—	Feed water temperature, °C
T_b	—	Remaining brine temperature, °C
T_o	—	Temperature of the brine leaving the preheater, °C
T_i	—	Temperature of the brine entering the preheater, °C
T_{cw}	—	Temperature of the brine in the condenser, °C
C_p	—	Specific heat at a constant pressure of seawater, kJ/kg·K
λ	—	Latent heat of evaporation, kJ/kg
A	—	Heat transfer area, m²
Q	—	Special heat consumption, kW
h	—	Heat transfer coefficient, W/m²·K
LMTD	—	Log mean temperature difference, °C
n	—	Number of the effect (the nth effect)

Subscripts

1	—	First effect
$i-1$	—	Previous effect
i	—	ith effect
in	—	Parameters entering the effect
out	—	Parameters leaving the effect
s	—	Steam
b	—	Brine
f	—	Feed
v	—	Vapor
p	—	Preheating process
e	—	Evaporation process
E	—	Evaporator
ph	—	Preheater
c	—	Condenser
t	—	Total

Acknowledgment

References

[1] D. Saldivia, C. Rosales, R. Barraza, L. Cornejo, Computational analysis for a multi-effect distillation (MED) plant driven by solar energy in Chile, Renewable Energy, 132 (2019) 206–220.

[2] N. Ghaffour, T.M. Missimer, G.L. Amy, Technical review and evaluation of the economics of water desalination: current and future challenges for better water supply sustainability, Desalination, 309 (2013) 197–207.

[3] B. Han, Z. Liu, H. Wu, Y. Li, Experimental study on a new method for improving the performance of thermal vapor compressors for multi-effect distillation desalination systems, Desalination, 344 (2014) 391–395.

[4] A.N.A. Mabrouk, Techno-economic analysis of tube bundle orientation for high capacity brine recycle MSF desalination plants, Desalination, 320 (2013) 24–32.

[5] P. Sharan, S. Bandyopadhyay, Energy optimization in parallel/cross feed multiple-effect evaporator based desalination system, Energy, 111 (2016) 756–767.

[6] I.S. Al-Mutaz, I. Wazeer, Comparative performance evaluation of conventional multi-effect evaporation desalination processes, Appl. Therm. Eng., 73 (2014) 1192–11201.

[7] H. El-Dessouky, I. Alatiqi, S. Bingulac, H. Ettouney, Steady-state analysis of the multiple effect evaporation desalination process, Chem. Eng. Technol., 21 (1998) 437–451.

[8] H.T. El-Dessouky, H.M. Ettouney, F. Mandani, Performance of parallel feed multiple effect evaporation system for seawater desalination, Appl. Therm. Eng., 20 (2000) 1679–1706.

[9] H.T. El-Dessouky, H.M. Ettouney, Multiple-effect evaporation desalination systems: thermal analysis, Desalination, 125 (1999) 259–276.

[10] M.A. Darwish, H.K. Abdulrahim, Feed water arrangements in a multi-effect desalting system, Desalination, 228 (2008) 30–54.

[11] R.K. Kamali, S. Mohebinia, Experience of design and optimization of multi-effects desalination systems in Iran, Desalination, 222 (2008) 639–645.

[12] A.O.B. Amer, Development and optimization of ME-TVC desalination system, Desalination, 249 (2009) 1315–1331.

[13] V.C. Onishi, R. Ruiz-Femenia, R. Salcedo-Díaz, A. Carrero-Parreño, J.A. Reyes-Labarta, E.S. Fraga, J.A. Caballero, Process optimization for zero-liquid discharge desalination of shale gas flowback water under uncertainty, J. Cleaner Prod., 164 (2017) 1219–1238.

[14] V.C. Onishi, A. Carrero-Parreño, J.A. Reyes-Labarta, R. Ruiz-Femenia, R. Salcedo-Díaz, E.S. Fraga, J.A. Caballero, Shale gas flowback water desalination: single vs multiple-effect evaporation with vapor recompression cycle and thermal integration, Desalination, 404 (2017) 230–248.

[15] M.A. Jamil, S.M. Zubair, Effect of feed flow arrangement and number of evaporators on the performance of multi-effect mechanical vapor compression desalination systems, Desalination, 429 (2018) 76–87.

[16] M.L. Elsayed, O. Mesalhy, R.H. Mohammed, L.C. Chow, Exergy and thermo-economic analysis for MED-TVC desalination systems, Desalination, 447 (2018) 29–42.

[17] M.L. Elsayed, O. Mesalhy, R.H. Mohammed, L.C. Chow, Performance modeling of MED-MVC systems: exergy-economic analysis, Energy, 166 (2019) 552–568.

[18] S. Zhou, Y. Guo, X. Mu, S. Shen, Effect of design parameters on thermodynamic losses of the heat transfer process in LT-MEE desalination plant, Desalination, 375 (2015) 40–47.

[19] S. Shen, Y. Guo, L. Gong, Analysis of heat transfer critical point in LT-MEE desalination plant, Desalination, 432 (2018) 64–71.

[20] I. Janghorban Esfahani, A. Ataei, K.V. Shetty, T.S. Oh, J.H. Park, C.K. Yoo, Modeling and genetic algorithm-based multi-objective optimization of the MED-TVC desalination system, Desalination, 292 (2012) 87–104.

[21] M. Ameri, M. Jorjani, Performance assessment and multi-objective optimization of an integrated organic Rankine cycle and multi-effect desalination system, Desalination, 392 (2016) 34–45.

[22] M. Ben Ali, L. Kairouani, Multi-objective optimization of operating parameters of a MSF-BR desalination plant using solver optimization tool of Matlab software, Desalination, 381 (2016) 71–83.

[23] H. Sayyaadi, A. Saffari, Thermoeconomic optimization of multi effect distillation desalination systems, Appl. Energy, 87 (2010) 1122–1133.

[24] H. Sayyaadi, A. Saffari, A. Mahmoodian, Various approaches in optimization of multi effects distillation desalination systems using a hybrid meta-heuristic optimization tool, Desalination, 254 (2010) 138–148.

[25] S.E. Shakib, M. Amidpour, C. Aghanajafi, A new approach for process optimization of a METVC desalination system, Desal. Water Treat. ,37 (2012) 84–96.

[26] V.K. Patel, R.V. Rao, Design optimization of shell-and-tube heat exchanger using particle swarm optimization technique, Appl. Therm. Eng., 30 (2010) 1417–1425.

[27] Y. Sun, W.D. Zeng, Y.F. Han, X. Ma, Y.Q. Zhao, Optimization of chemical composition for TC11 titanium alloy based on artificial neural network and genetic algorithm, Comput. Mater. Sci., 50 (2011) 1064–1069.

[28] T. Nazghelichi, M. Aghbashlo, M.H. Kianmehr, Optimization of an artificial neural network topology using coupled response surface methodology and genetic algorithm for fluidized bed drying, Comput. Electron. Agric., 75 (2011) 84–91.

[29] A. Konak, D.W. Coit, A.E. Smith, Multi-objective optimization using genetic algorithms: a tutorial, Reliab. Eng. Syst. Saf., 91 (2006) 992–1007.

[30] I.H. Yilmaz, M.S. Söylemez, Design and computer simulation on multi-effect evaporation seawater desalination system using hybrid renewable energy sources in Turkey, Desalination, 291 (2012) 23–40.

[31] P. Palenzuela, A.S. Hassan, G. Zaragoza, D.C. Alarcón-Padilla, Steady state model for multi-effect distillation case study: Plataforma Solar de Almería MED pilot plant, Desalination, 337 (2014) 31–42.

[32] P. Druetta, P. Aguirre, S. Mussati, Optimization of Multi-Effect Evaporation desalination plants, Desalination, 311 (2013) 1–15.

[33] M. Papapetrou, A. Cipollina, U. La Commare, G. Micale, G. Zaragoza, G. Kosmadakis, Assessment of methodologies and data used to calculate desalination costs, Desalination, 419 (2017) 8–19.

[34] A.M. El-Nashar, Economics of small solar-assisted multiple-effect stack distillation plants, Desalination, 130 (2000) 201–215.

[35] G. Kosmadakis, M. Papapetrou, B. Ortega-Delgado, A. Cipollina, D.C. Alarcón-Padilla, Correlations for estimating the specific capital cost of multi-effect distillation plants considering the main design trends and operating conditions, Desalination, 447 (2018) 74–83.

[36] Y. Wang, N. Lior, Thermoeconomic analysis of a low-temperature multi-effect thermal desalination system coupled with an absorption heat pump, Energy, 36 (2011) 3878–3887.

[37] M.A. Jamil, S.M. Zubair, On thermoeconomic analysis of a single-effect mechanical vapor compression desalination system, Desalination, 420 (2017) 292–307.

[38] K. Deb, A. Pratap, S. Agarwal, T. Meyarivan, A fast and elitist multiobjective genetic algorithm: NSGA-II, IEEE Trans. Evol. Comput., 6 (2002) 182–197.